GEBZE TECHNICAL UNIVERSITY

Acta Materialia Turcica

Volume 6, April 2022, Pages 1-11

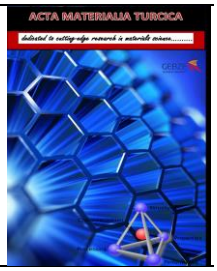

Effect of Mild Steel Particles on the Thermal, Frictional and Wear Characteristics of Ceramic Matrix Composites

STEPHEN DUROWAYE*, OLUWATOMISIN AWOTUNDE, SAMUEL ALAO, DIANA KANU

Department of Metallurgical and Materials Engineering, University of Lagos, Nigeria

Abstract:

Micro particles of mild steel, silicon carbide, magnesia and bentonite were employed as input materials in the production of ceramic matrix composites by powder metallurgy. The composites were characterised and they demonstrated desirable characteristics. Sample D containing 12 wt. % of mild steel particles exhibited a very good thermal stability in the temperature range of 0 – 800 ^{0}C, high coefficient of friction of 0.59 and reduced wear rate of 2.228 x 10^{-5} g/m which implies high resistance to wear. Proper blending of constituent materials and strong bonding enhanced the characteristics of the composites. The results indicated the suitability of the composite for use in fields that require high resistance to thermal decomposition and wear.

Keywords: Ceramic matrix composites, Micro particles, Thermal decomposition, Friction, Wear rate.

1. INTRODUCTION

The need for the development of friction materials that will exhibit superlative characteristics especially high resistance to thermal decomposition and wear cannot be over emphasized. This is because of the immense benefits, which such materials will offer. Ceramics are suitable materials for wear resistance components because of their hardness, corrosion resistance, and high thermal stability, which have made them to be extensively used for tribological applications [1]. Generally, the performance of materials under different operating conditions is influenced by the composition, structure, interfaces, grain size, and properties of constituents such as hardness, mechanical strength, wear resistance, and thermal conductivity [2, 3].

The high hardness and abrasion resistance of silicon carbide (SiC) have made carbon fiber/SiC composites the choice materials for frictional purposes. They exhibit superlative characteristics such as high coefficient of friction, high resistance to wear and corrosion, heat resistance as they can function very well at temperatures up to 1200 °C, low density, low coefficient of linear thermal expansion, and the absence of noise during braking [4]. Because of these desirable characteristics, they are widely used in the brake systems of automobiles and aircrafts. Materials made of ceramic composites which are used in various applications experience mechanical abrasion and thermal wear in service. Wear and coefficient of friction represent interface instability that have effect on the life span of friction materials under contact and repeated cyclic motion. They could be indirect measure of contact surface degradation that affects materials quality [3]. Friction is the resistance to movement when a solid surface moves over another surface. The two surfaces that are rubbing against each other experience deformation/degradation [1]. For example, brake pads must have a sufficiently high coefficient of friction with the brake disc to achieve braking effectiveness and should not decompose at high temperature so that the coefficient of friction with the brake disc is not adversely affected/reduced [5, 6].

Generally, wear control is challenging due to some factors such as environment (temperature, humidity, oxygen content), contact (normal load, sliding speed, type of motion), and materials properties such as hardness, surface roughness, contaminations, porosity and interfacial bonding of constituents [7]. However,

* Corresponding Author: durosteve02@yahoo.com
Tel.: +234 8036844029

Acta Materialia Turcica

Volume 6, April 2022, Pages 1-11

ceramic matrix composites were developed to solve the problems of wear and thermal decomposition. Ceramic matrix composites dispersed with metallic particles are among the materials that have potentials for high functional applications under severe environment such as high temperature. These composites offer the possibility of combining resistance to heat, wear and corrosion because of the ceramic phase with mechanical strength offered by the presence of metallic phase [8]. The oxidation behaviour of Zirconia matrix composite dispersed with stainless steel particles was investigated. The result indicated that the ceramic composite exhibited a different corrosion behaviour at 700 ^{0}C and 800 ^{0}C compared to pure stainless steel because of the presence of Zirconia [8]. Carbon fiber reinforced silicon carbide matrix composites were developed by liquid-phase siliconizing technology for energy intensive brake system application. The results indicated that the composites demonstrated a relatively high coefficient of friction and minimal wear rate [4]. Hence, this study seeks to investigate the effect of mild steel particles on the thermal, frictional and wear characteristics of ceramic matrix composites for possible application in areas that require high heat and wear resistance.

2. MATERIALS AND METHODS

2.1 Materials and Preparation

Silicon carbide, mild steel particles, bentonite and magnesia are the input materials. Mild steel chips obtained from the Engineering workshop of the University of Lagos were ground and sieved to the desired particles size using British standardised sieves (BSS). As-received particles of silicon carbide, magnesia and bentonite were obtained in Lagos. Figure 1 shows the materials used.

Figure 1. Input materials used for the study (a) mild steel chips (b) 105-µm ground and sieved mild steel particles (c) As-received 53-µm silicon carbide (d) As-received 90-µm bentonite (e) As-received 90-µm magnesia.

2.2 Production of the Composites

105-µm mild steel particles were blended with 53-µm silicon carbide, 90-µm magnesia and 90-µm bentonite. Varied formulations were used in producing the samples as illustrated in Table 1. Phenolic resin and water were mixed with each of the formulations. The mixtures were fed into metal moulds rubbed with oil and pressed at 0.35 MPa to enhance their surface smoothness. The samples were removed from the moulds and sun-dried for 12 hrs. They were oven dried at 110 ^{0}C for 12 hrs to avoid cracking during sintering. They were sintered at 1100 ^{0}C using a muffle furnace and soaked for 1 hr after which they were taken out of the furnace and allowed to cool. Few samples are presented (Figure 2).

* Corresponding Author: durosteve02@yahoo.com
Tel.: +234 8036844029

Acta Materialia Turcica

Volume 6, April 2022, Pages 1-11

Table 1. Proportion of used materials (wt. %).

Sample	Mild steel particles	Silicon carbide	Magnesia	Bentonite	Phenolic resin	Total
A	0	30	40	25	5	100
B	4	35	31	25	5	100
C	8	40	22	25	5	100
D	12	45	13	25	5	100
E	16	50	4	25	5	100

Figure 2. Photograph of some of the ceramic composite samples produced.

Figure 3. Experimental set-up of the flame resistance test on the composites.

2.3 Characterisation of the Samples

A scanning electron microscope was employed to reveal the microstructure of the samples. To test for the flame resistance of the composites, each of the five samples was weighed before the test and their initial weights were recorded. They were put on wire gauze placed directly on the flame of a Bunsen burner for one hour. The flame was removed and the samples were left to cool and their final weights were recorded. The weight loss obtained is presented in Table 3. The experimental set-up for this test is shown in Figure 3.

Thermogravimetric method was used in determining the thermal stability of the samples with the aid of a thermogravimetric analyser. The analyser measured the weight of the samples as they were heated at varied temperatures. The onset temperature of destruction (T_{des}) of the samples, which indicates their decomposition temperature was recorded. The coefficient of friction of the samples was determined by making them slide over a smooth mild steel plane inclined at 35^0 that had a pulley with loads applied on the hanger. The coefficient of friction (μ) between each sample and the steel surface was determined by employing Equations 1 and 2 [9].

$$\mu = \frac{\text{Sliding force}}{\text{Normal force}} \qquad 1$$

$$\mu = \frac{P - W\sin\theta}{W\cos\theta} \qquad 2$$

Where:
P = Load on the hanger (N)

* Corresponding Author: durosteve02@yahoo.com
Tel.: +234 8036844029

Acta Materialia Turcica

Volume 6, April 2022, Pages 1-11

W = Weight of sample (N)
θ = Angle of inclination

Dry sliding abrasive wear test was conducted by employing a pin-on-disc wear tester according to ASTM standard G99. The disc rotated with the aid of a D.C. motor of speed 250 rpm and sliding occurred between the stationary samples that had contact with the rotating disc. The wear rate (ω) was calculated using Equations 3 – 5 [10].

$$\text{Wear rate } (\omega) = \frac{\Delta w}{s} \qquad 3$$

Where:

$$\Delta w = w_0 - w_1 \qquad 4$$

$$S = \text{sliding speed} = 2\pi NDt = 1256.8 \text{ m} \qquad 5$$

Δw = weight loss in g
w_0 = initial weight of sample before wear in g
w_1 = final weight of sample after wear in g
D = diameter of the grit sandpaper which is 0.16 m
N = number of revolution per minute (rpm) of the pin-on disc which is 250
t = exposure time to wear = 5 mins
π = 3.142.

3. RESULTS AND DISCUSSION

3.1 Microstructure

The microstructures show that the samples contain different phases with different shapes. Some are globular while some are needle-like as revealed in the micrographs. The elemental composition as revealed by the energy-dispersive spectroscopy (EDS) spectra show that sample A contains O, Si, Al, Mg and Ca. Other samples also contain these elements plus Fe from added iron mild steel particles shown in Figure 4 – 8. The whitish area in the micrographs is magnesia (MgO) phase while the dark area is silicon carbide phase and gray is a combination of Fe and bentonite phase.

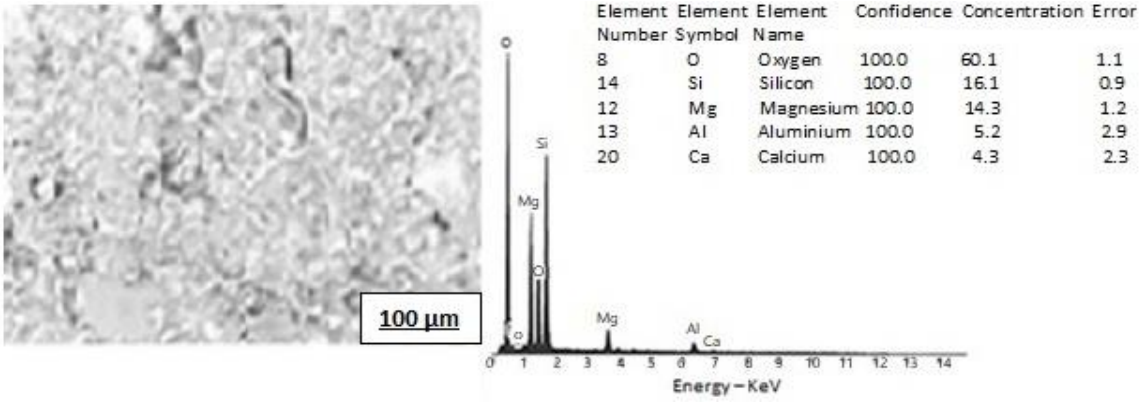

Element Number	Element Symbol	Element Name	Confidence	Concentration	Error
8	O	Oxygen	100.0	60.1	1.1
14	Si	Silicon	100.0	16.1	0.9
12	Mg	Magnesium	100.0	14.3	1.2
13	Al	Aluminium	100.0	5.2	2.9
20	Ca	Calcium	100.0	4.3	2.3

Figure 4. Scanning electron micrograph (SEM) of sample A with the EDS spectrum showing the phases and the elemental composition.

* Corresponding Author: durosteve02@yahoo.com
Tel.: +234 8036844029

Acta Materialia Turcica

Volume 6, April 2022, Pages 1-11

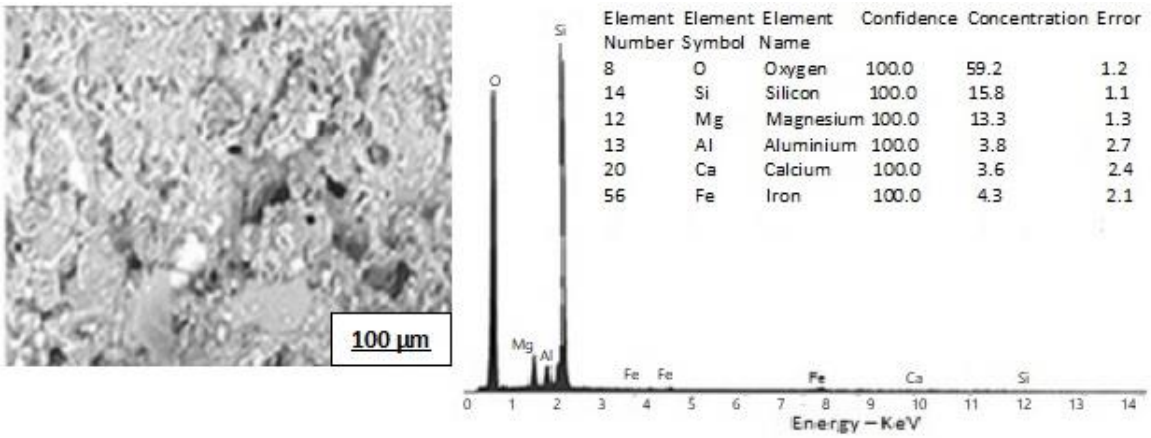

Element Number	Element Symbol	Element Name	Confidence	Concentration	Error
8	O	Oxygen	100.0	59.2	1.2
14	Si	Silicon	100.0	15.8	1.1
12	Mg	Magnesium	100.0	13.3	1.3
13	Al	Aluminium	100.0	3.8	2.7
20	Ca	Calcium	100.0	3.6	2.4
56	Fe	Iron	100.0	4.3	2.1

Figure 5. Scanning electron micrograph (SEM) of sample B with the EDS spectrum showing the phases and the elemental composition.

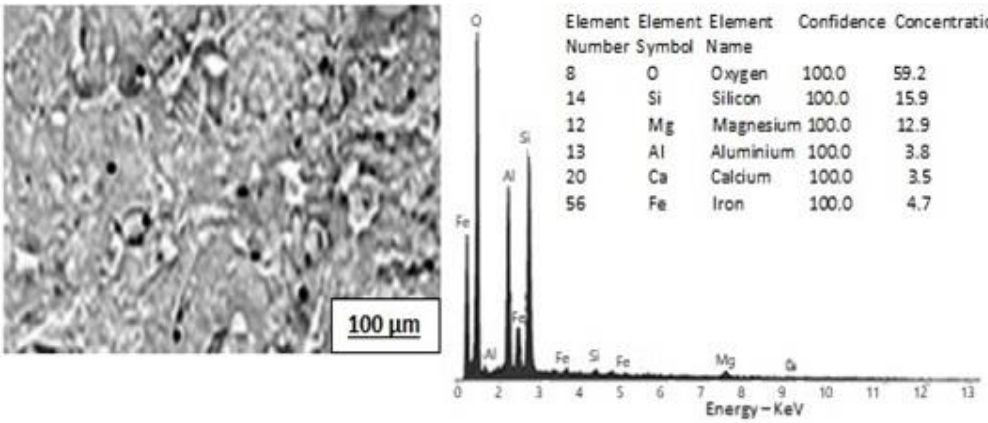

Element Number	Element Symbol	Element Name	Confidence	Concentration	Error
8	O	Oxygen	100.0	59.2	1.3
14	Si	Silicon	100.0	15.9	1.4
12	Mg	Magnesium	100.0	12.9	1.3
13	Al	Aluminium	100.0	3.8	2.6
20	Ca	Calcium	100.0	3.5	2.5
56	Fe	Iron	100.0	4.7	2.3

Figure 6. Scanning electron micrograph (SEM) of sample C with the EDS spectrum showing the phases and the elemental composition.

* Corresponding Author: durosteve02@yahoo.com
Tel.: +234 8036844029

Acta Materialia Turcica

Volume 6, April 2022, Pages 1-11

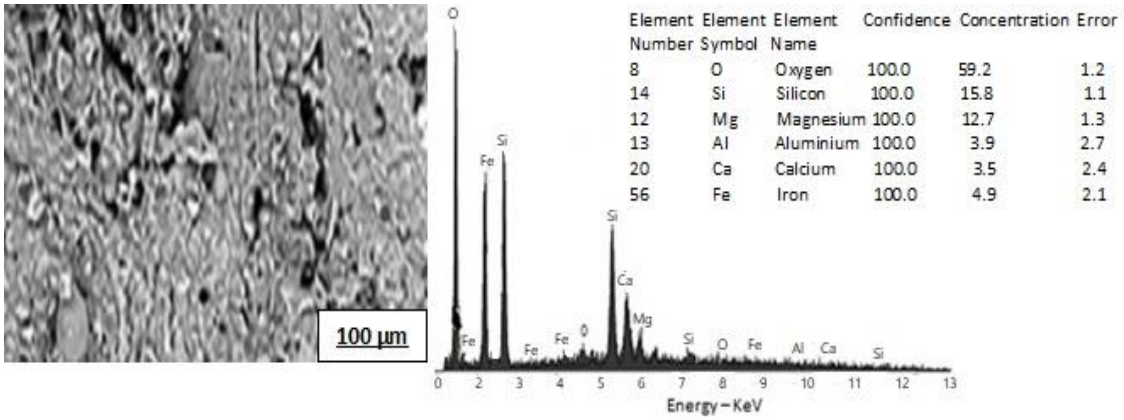

Element Number	Element Symbol	Element Name	Confidence	Concentration	Error
8	O	Oxygen	100.0	59.2	1.2
14	Si	Silicon	100.0	15.8	1.1
12	Mg	Magnesium	100.0	12.7	1.3
13	Al	Aluminium	100.0	3.9	2.7
20	Ca	Calcium	100.0	3.5	2.4
56	Fe	Iron	100.0	4.9	2.1

Figure 7. Scanning electron micrograph (SEM) of sample D with the EDS spectrum showing the phases and the elemental composition.

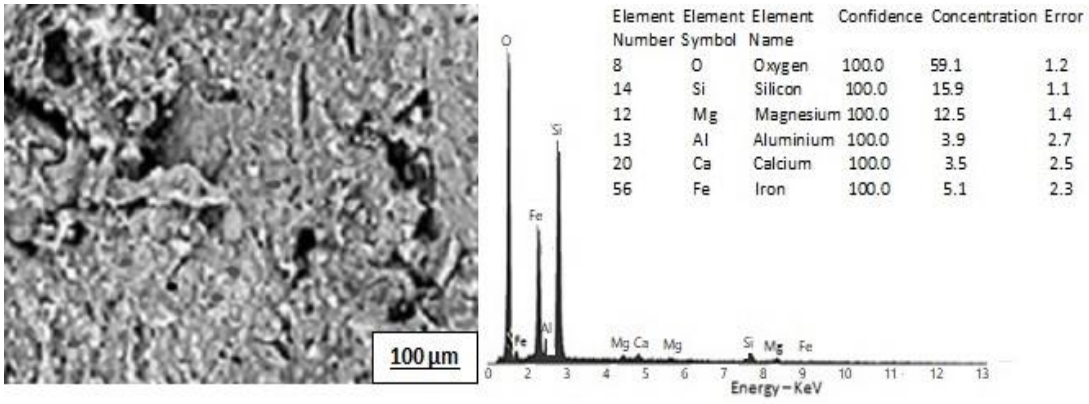

Element Number	Element Symbol	Element Name	Confidence	Concentration	Error
8	O	Oxygen	100.0	59.1	1.2
14	Si	Silicon	100.0	15.9	1.1
12	Mg	Magnesium	100.0	12.5	1.4
13	Al	Aluminium	100.0	3.9	2.7
20	Ca	Calcium	100.0	3.5	2.5
56	Fe	Iron	100.0	5.1	2.3

Figure 8. Scanning electron micrograph (SEM) of sample E with the EDS spectrum showing the phases and the elemental composition.

3.2 Heat Resistance of the Samples

After 1 hr of exposing (Figure 3) the samples to heat, the initial weight of the samples before exposure to heat was the same as the final weight after exposure except sample A. Sample A lost 0.01 g which is 0.015 %. This shows that 99.9 % of the weight of samples A was retained but 100 % of the weight of samples B, C, D and E was retained indicating that there was no weight loss in them. It implies that the samples demonstrated excellent resistance to thermal decomposition, which may be because of the refractory nature of ceramics and the strong bond existing between the particles.

* Corresponding Author: durosteve02@yahoo.com
Tel.: +234 8036844029

Acta Materialia Turcica

Volume 6, April 2022, Pages 1-11

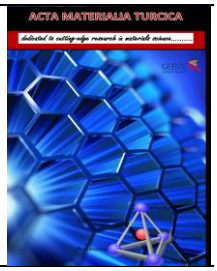

Table 2. Effect of heat on the samples.

Sample	Description	Initial Weight (g)	Final Weight (g)	Weight loss (g)	Weight loss (%)	Weight Retained (%)
A	Not mixed with mild steel particles	67.17	67.18	0.01	0.015	99.985
B	Mixed with 4 wt. % mild steel particles	156.51	156.51	-	-	100
C	Mixed with 8 wt. % mild steel particles	158.09	158.09	-	-	100
D	Mixed with 12 wt. % mild steel particles	159.75	159.75	-	-	100
E	Mixed with 16 wt. % mild steel particles	162.23	162.23	-	-	100

Furthermore, results of the thermogravimetric test show that the weight loss due to thermal decomposition is minimal as illustrated in Figure 9. Sample A demonstrated 0.45 % loss in weight, which is higher than that of others. Specifically, sample D demonstrated the least loss in weight of 0.24 %. Thermal decomposition started from 800 ^{0}C (onset) to the peak (1100 ^{0}C) with reduction in weight of the samples. The weight loss of the samples is in the range of 0.24 – 0.45 %. This is very low and it indicates that the composites exhibited high resistance to thermal decomposition, which may be because of the refractory nature of ceramics and the strong bond existing between the particles. The strong bond existing between the particles served as a shield against thermal decomposition, which agrees with the report by [11].

* Corresponding Author: durosteve02@yahoo.com
Tel.: +234 8036844029

Acta Materialia Turcica

Volume 6, April 2022, Pages 1-11

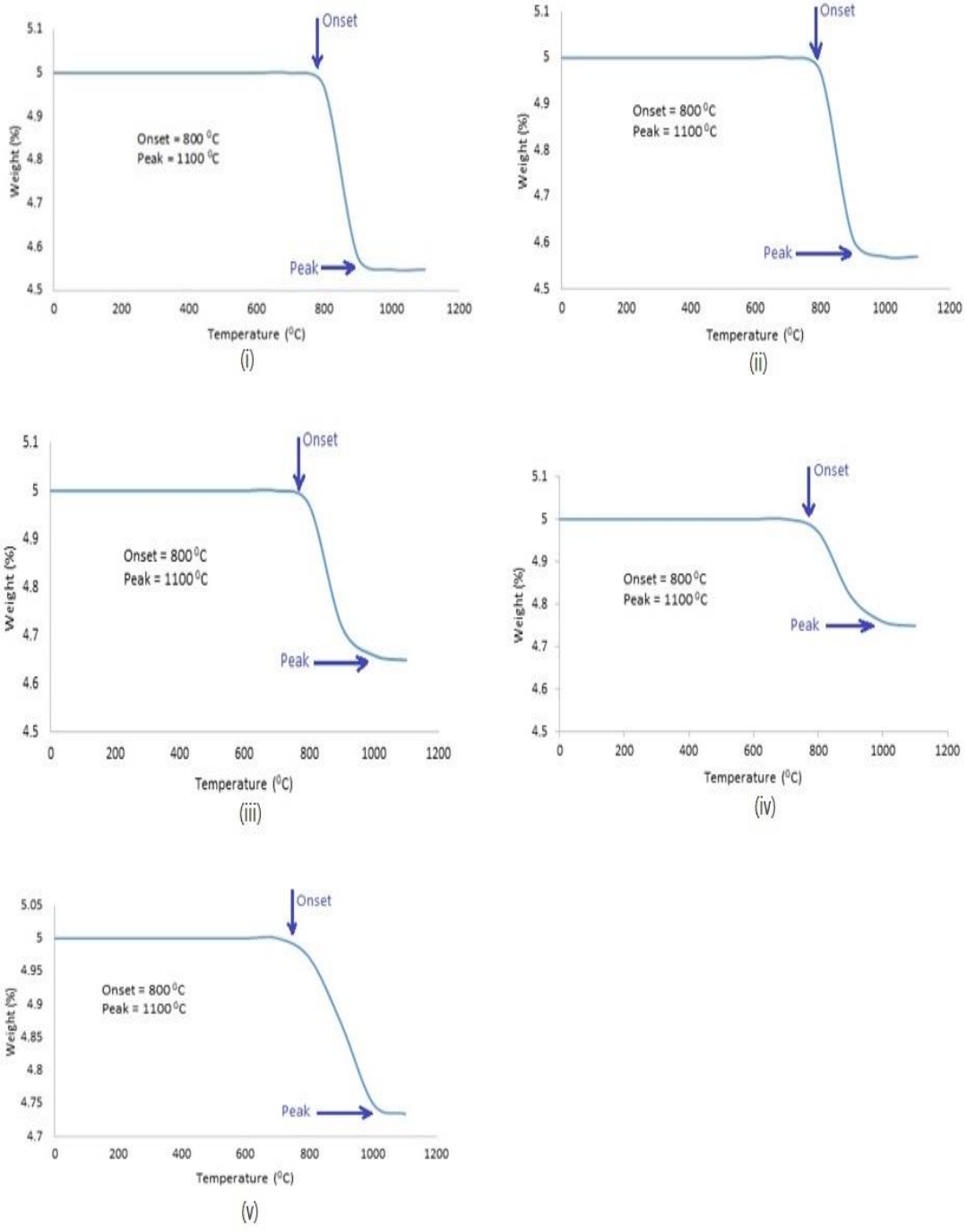

Figure 9. Thermogravimetric plot of the samples showing the decomposition temperatures (onset and peak) and the weight (i) sample A, (ii) sample B, (iii) sample C, (iv) sample D, (v) sample E.

* Corresponding Author: durosteve02@yahoo.com
Tel.: +234 8036844029

Acta Materialia Turcica

Volume 6, April 2022, Pages 1-11

3.3 Coefficient of Friction

As shown in Figure 10, there is a progressive increase in the coefficient of friction (μ) of the samples. This shows that asperities exist between the surfaces of the mild steel and the samples. The rise in coefficient of friction is promoted by the rising weight of samples. The range of the coefficient of friction which is 0.52 – 0.59, is more than the specification range (0.3 – 0.38) for automobiles brake linings/pads by the Nigerian industrial standard [12] which is a positive development.

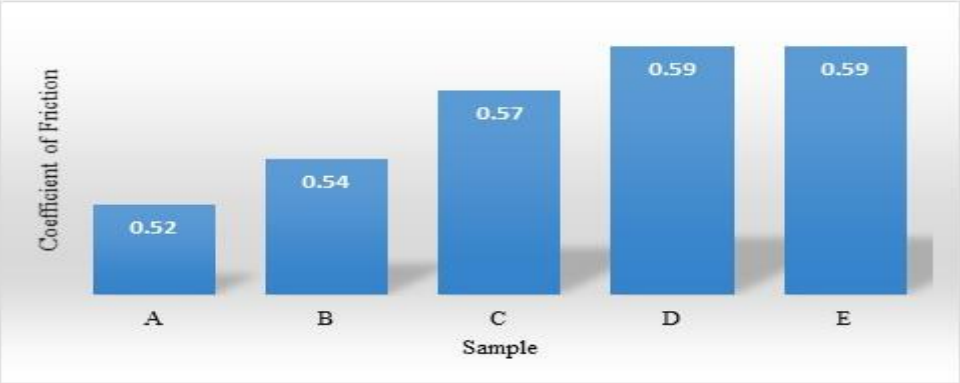

Figure 10. Coefficient of friction of the samples.

3.4 Loss in Weight and Wear Rate of the samples

The samples experienced loss in weight because of surface deformation due to ploughing force of asperities as presented in Figure 11. A similar submission was reported by [13]. The same trend is seen in Figure 12 since weight loss and wear rate are directly related. Samples D and E exhibited the lowest wear rate (2.228 x 10^{-5} g/m). The strong bond existing between the particles reduced the possibility of particles pullout and led to the reduced wear rate of the samples.

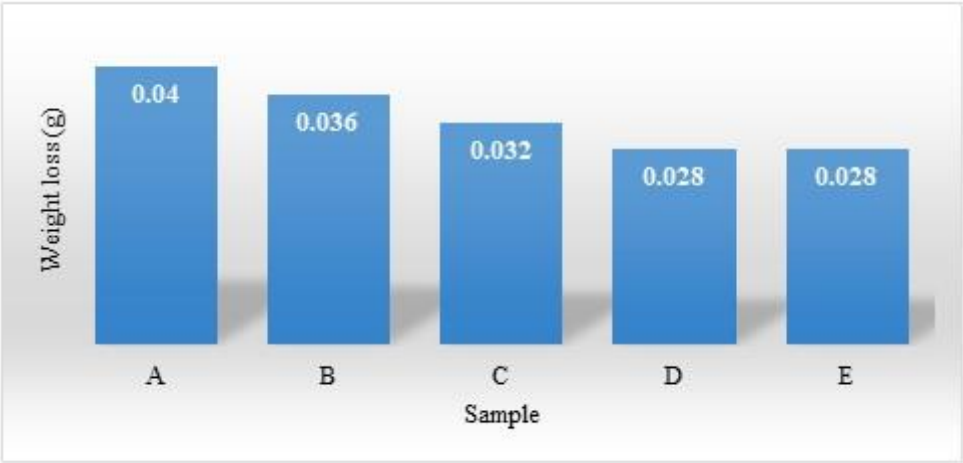

Figure 11. Loss in weight due to wear of the samples.

* Corresponding Author: durosteve02@yahoo.com
Tel.: +234 8036844029

Acta Materialia Turcica

Volume 6, April 2022, Pages 1-11

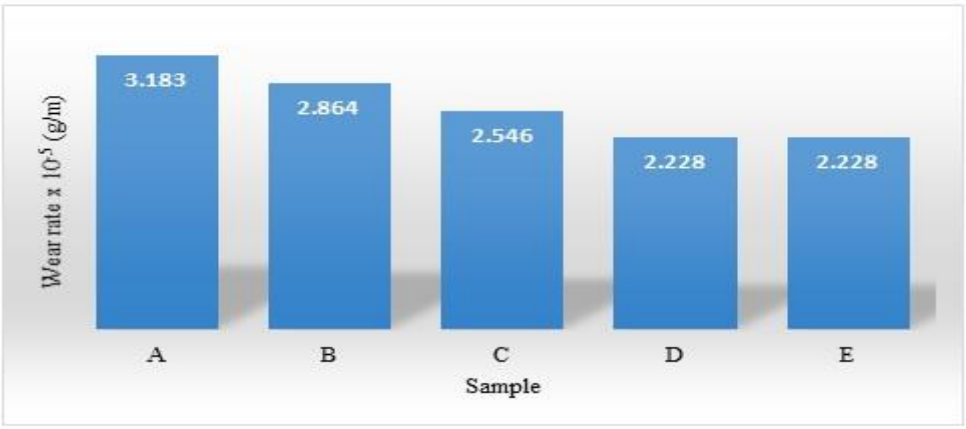

Figure 12. Wear rate of the samples.

4. CONCLUSION

Particulate ceramic matrix composites were produced and characterised. The composites demonstrated very good properties. Sample D did not experience any weight loss when heated for 1 hr and exhibited no decomposition in the temperature range of 0 – 800 ^{0}C. It also exhibited a high coefficient of friction of 0.59 and minimal wear rate of 2.228 x 10^{-5} g/m. These indicate that the sample demonstrated high thermal stability/heat resistance and wear resistance.

Conflict of Interests

The authors declare no conflict of interest.

Declaration of Ethical Standards

The authors of this article declare that the materials and methods used in this study do not require ethical committee permission and/or legal-special permission.

REFERENCES

[1] A.E. Pramono, M.Z. Nura, J.W.M. Soedarsonob, N. Indayaningsih, Properties of wear rate and electrical conductivity of carbon ceramic composites, Journal of Ceramic Processing Research. 20(1) (2019) 1-7.

[2] W.Z. Eddine, P. Matteazzi, J.P. Celis, Mechanical and tribological behaviour of nanostructured copper-alumina cermet obtained by pulsed electric current sintering. Wear 297 (2013) 762-773.

[3] R. Riina, A. Maksim, V. Renno, H. Simo-Pekka, Comparison of the wear and frictional properties of Cu matrix composites prepared by pulsed electric current sintering, Proceedings of the Estonian Academy of Sciences. **63**(1) (2014) 62-74.

[4] A.P. Garshina, V.I. Kulik, A.S. Nilov, Study of ceramic-matrix composites tribological properties paired with cermet, Elsevier, Procedia Engineering. 206 (2017) 771-776.

[5] M. Djafri, M. Bouchetara, C. Busch, S. Weber, Experimental study of the tribological behaviour of materials of brake, MECHANIKA. 20(4) (2014) 420-425.

[6] K.K. Ikpambese, D.T. Gundu, L.T. Tuleun, Evaluation of palm kernel fibers (PKFs) for production of asbestos-free automotive brake pads, Journal of King Saud University – Engineering Sciences. 28 (2016) 110-118.

[7] K. Holmberg, A. Matthews, Coatings Tribology, Properties, Mechanisms, Techniques and Applications in Surface Engineering (Briscoe, B., ed.). Tribology

* Corresponding Author: durosteve02@yahoo.com
Tel.: +234 8036844029

Acta Materialia Turcica

Volume 6, April 2022, Pages 1-11

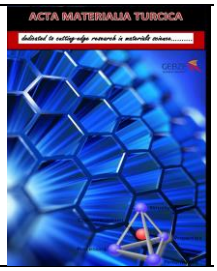

and Interface Engineering, 2nd edition, Series 56, 2009.
[8] J. Tarabay, V. Peres, E. Serris, F. Valdivieso, M. Pijolat, Zirconia matrix composite dispersed with stainless steel particles: processing and oxidation behaviour, Elsevier, Journal of the European Ceramic Society. 33 (2013) 1101-1110.

[9] U.K. Essays, Experiment to Determine the Coefficient of Friction, SAE Automotive Engineers Congress. Society of Automotive Engineers, Paper Number 670146, Detroit, USA. 2018. https://www.ukessays.com/essays/physics/experiment-determine coefficient4293.php? vref=1,

[10] A.I. Olabisi, N.A. Ademoh, O.M. Okechukwu, Development and assessment of composite brake pad using pulverized cocoa beans shells filler, International Journal of Materials Science and Applications. 5(2) (2016) 66-78.

[11] A. Subasinghe, R. Das, D. Bhattacharyya, Study of thermal, flammability, and mechanical properties of intumescent flame retardant pp/kenaf nanocomposites, Taylor & Francis Group, International Journal of Smart and Nano Materials. 7(3) (2016) 202-220.

[12] Nigerian Industrial Standards, Specification for friction materials for road vehicles brake lining and pads, Standard Organisation of Nigeria (SON), NIS 323, Nigeria, 1997.

[13] D.S. Yawas, S.Y. Aku, S.G. Amaren, Morphology and properties of periwinkle shell asbestos-free brake pad, Journal of King Saud University – Engineering Sciences. 28 (2016) 103-109.

* Corresponding Author: durosteve02@yahoo.com
Tel.: +234 8036844029